UDC 621.397.132
778.633
535.6.08

BBC

RESEARCH DEPARTMENT

REPORT

A note on dichroic gratings for colour encoding

No. 1972/32

Research Department, Engineering Division
THE BRITISH BROADCASTING CORPORATION

RESEARCH DEPARTMENT

A NOTE ON DICHROIC GRATINGS FOR COLOUR ENCODING

Research Department Report No. **1972/32**
UDC 621.397.132
778.633
535.6.08

This Report may not be reproduced in any form without the written permission of the British Braadcasting Corporation.

It uses SI units in accordance with B.S. document PD 5686.

K. Hacking, B.Sc.

Head of Research Department

(PH-93)

Research Department Report No. 1972/32

A NOTE ON DICHROIC GRATINGS FOR COLOUR ENCODING

September 1972

Research Department Report No. 1972/32
UDC 621.397.132
778.633
535.6.08

A NOTE ON DICHROIC GRATINGS FOR COLOUR ENCODING

Summary

The information-encoding action of a pair of dichroic gratings (sometimes known as striped filters) is analysed in general terms, using the effect on the spatial-frequency spectrum of the image of a scene to reveal their intrinsic properties. Two colour-television camera systems based on a single pick-up tube are discussed, and an attempt is made to assess the physical tolerances required in the construction of suitable dichroic gratings for this application. Finally, several technological processes which might be used to construct gratings with multilayer dielectric coatings are mentioned.

1. Introduction

Several colour camera systems have been developed recently which make use of the information-encoding properties of dichroic optical gratings. The gratings take the form of transparent, regular stripes alternating in transmitted colour and are placed in a real image plane. In one system for a single-tube colour television camera,[1] developed by R.C.A., two such dichroic gratings are used in tandem. The transmission colours are yellow-and-white (clear) for one grating and cyan-and-white for the other, corresponding to a spatial encoding of blue and red information respectively. In the ABTO process[2] for photographic recording on black-and-white film, colour image encoding is achieved by means of three crossed gratings, one for each of the three primary colours.

The most efficient dichroic gratings are expected to be those in which the colour alternation is obtained by forming stripes of multilayer dielectric materials on a glass substrate. The general characteristics of multilayer interference filters, and their design for colour telecine and three-tube camera equipment, are now well known. A new problem in making the filters arises, however, if we further require the multilayer coating to be formed as a grating of very narrow but regularly spaced stripes. The difficulty increases considerably if the line spacing is small, less than 100 μm say, and in this case new constructional techniques may need to be developed. The manufacturing difficulties will depend, also, on the performance tolerances required for such features as line parallelism, spacing regularity and uniformity of spectral characteristics.

The purpose of this note is threefold:

(1) To analyse the encoding action of a pair of dichroic gratings suitable for a single-tube colour television camera

(2) To estimate the tolerance requirements of the grating parameters in relation to the methods of information retrieval discussed

(3) To suggest approaches to the technological problem of grating construction using multilayer dielectric materials.

2. Analysis of dichroic gratings in tandem

We can describe the variation in the transmission coefficient of a single periodic grating by an infinite Fourier series. For example, using the formal complex notation,

and with reference to a rectangular set of axes* (x, y) as shown in Fig. 1,

$$T(x,y,\lambda) = \sum_{n=-\infty}^{n=\infty} \alpha_n(\lambda) \exp[j\,2\pi n\,(px + qy)] \qquad (1)$$

where $T(x,y,\lambda)$ = transmission coefficient

λ = spectral wavelength

n = integer

$j = \sqrt{-1}$

α_n = amplitudes of Fourier components for wavelength λ

$p = Z \cos\theta$ = spatial frequency of grating in x direction

$q = Z \sin\theta$ = spatial frequency of grating in y direction

Z = maximum spatial frequency of grating

θ = angle between the grating stripes and the y axis

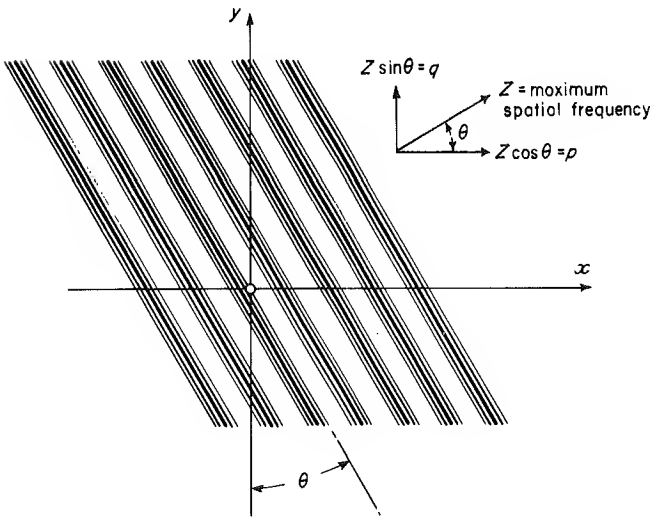

Fig. 1 - Notation for a single periodic grating

It should be noted that the Fourier coefficients, $\alpha_n(\lambda)$, are functions of the wavelength of the incident radiation. This is, of course, the particular feature of a dichroic grating which distinguishes it from an ordinary (black-and-white) grating. Hence the effective transmission profile of the grating over a band of radiation is determined by integration with respect to wavelength. The most important Fourier coefficient is that of the fundamental component $\alpha_1(\lambda)$ and this is designed to vary with wavelength according to the colorimetric requirements of the system; normally, the coefficient is arranged to be zero outside a selected spectral waveband.

Considerable simplification in the analysis arises by now assuming that the spatial bandwidth of the scene to be encoded is sufficiently well limited, so that no serious 'aliasing' or intermodulation effects occur with the harmonics of the grating spectrum. Thus, by ignoring coefficients of order n>1 in Equation (1) and by selecting a suitable origin of co-ordinates the effective transmission coefficient can be described in the simpler form

$$T(x,y,\lambda) = A(\lambda) + B(\lambda) \cos 2\pi(px + qy) \qquad (2)$$

where $A(\lambda)$ is the mean value to T with respect to x,y and $B(\lambda)$ is the amplitude of the variation of the fundamental component, which is proportional to $(T_{max} - T_{min})$.

Extending the description, for two gratings in tandem we obtain the combined transmission coefficient.

$$T_1(x,y,\lambda)T_2(x,y,\lambda) = [A_1(\lambda) + B_1(\lambda) \cos 2\pi(p_1x + q_1y)] \times [A_2(\lambda) + B_2(\lambda) \cos 2\pi(p_2x + q_2y)] \qquad (3)$$

where subscripts 1 and 2 denote the two gratings, respectively.

Expanding the R.H.S. of Equation (3)

$$\begin{aligned} T_1(x,y,\lambda)T_2(x,y,\lambda) = {} & A_1(\lambda)\,A_2(\lambda) \\ & + A_2(\lambda)\,B_1(\lambda) \cos[2\pi(p_1x + q_1y)] \\ & + A_1(\lambda)\,B_2(\lambda) \cos[2\pi(p_2x + q_2y)] \\ & + \tfrac{1}{2}B_1(\lambda)\,B_2(\lambda) \cos\{2\pi[(p_1 + p_2)x + (q_1 + q_2)y]\} \\ & + \tfrac{1}{2}B_1(\lambda)\,B_2(\lambda) \cos\{2\pi[(p_1 - p_2)x + (q_1 - q_2)y]\} \end{aligned} \qquad (4)$$

The (low order) spatial-frequency spectrum of the combined gratings is easily constructed using Equation (4). For example, Fig. 2 shows a two-dimensional frequency diagram for the general case $p_1 \neq p_2$ and $q_1 \neq q_2$, using arbitrary values of p and q.

The modulating effect of the combined gratings on the focussed image of a scene is shown by the frequency diagram in Fig. 3, where the area enclosed by the dashed-line around the origin is arbitrarily chosen to represent the extent of the spatial-frequency spectrum of the scene alone. It will be observed that translated replicas of the scene spectrum (although of different magnitudes) appear centred on each frequency component of the grating spectrum. By analogy with electrical modulation concepts, the major components of the grating spectra are spatial frequency 'carriers'.

In order to achieve satisfactory signal encoding for a colour reproduction system, we require that

(1) the magnitudes of the two principal carriers and the d.c. component (including their associated sidebands)

* The convention in which the x-axis corresponds to the horizontal line-scan direction is used throughout this report.

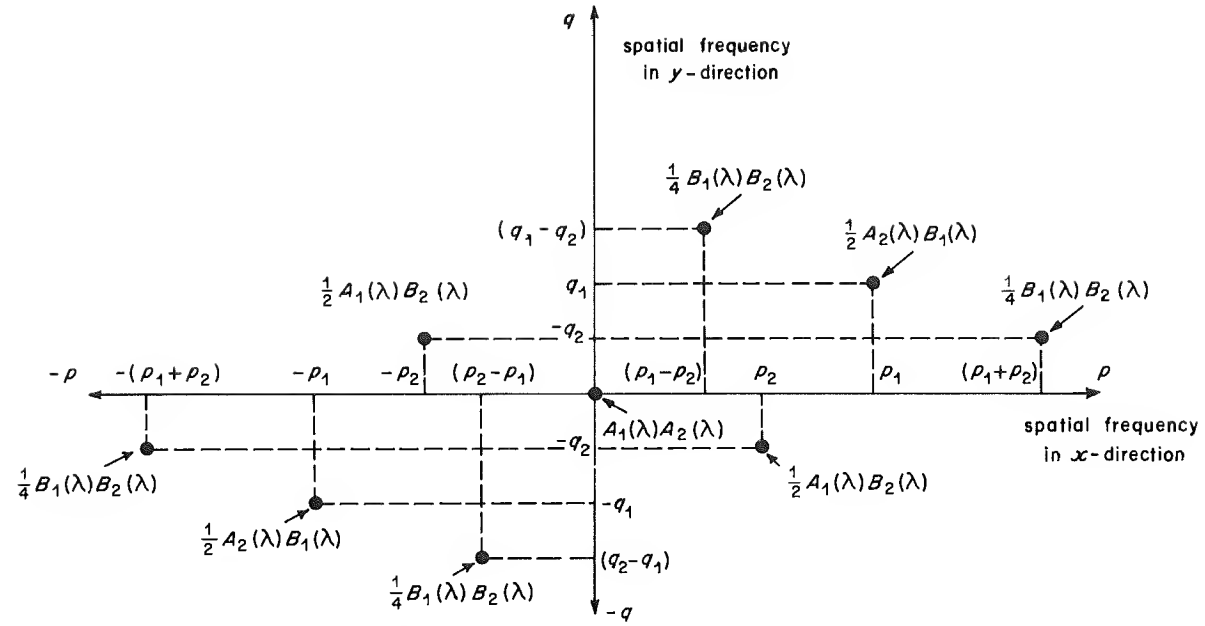

Fig. 2 - Spatial-frequency spectrum of two gratings in tandem: general case using arbitrary values of p_1, q_1 and p_2, q_2. Amplitudes of spectral components are as indicated

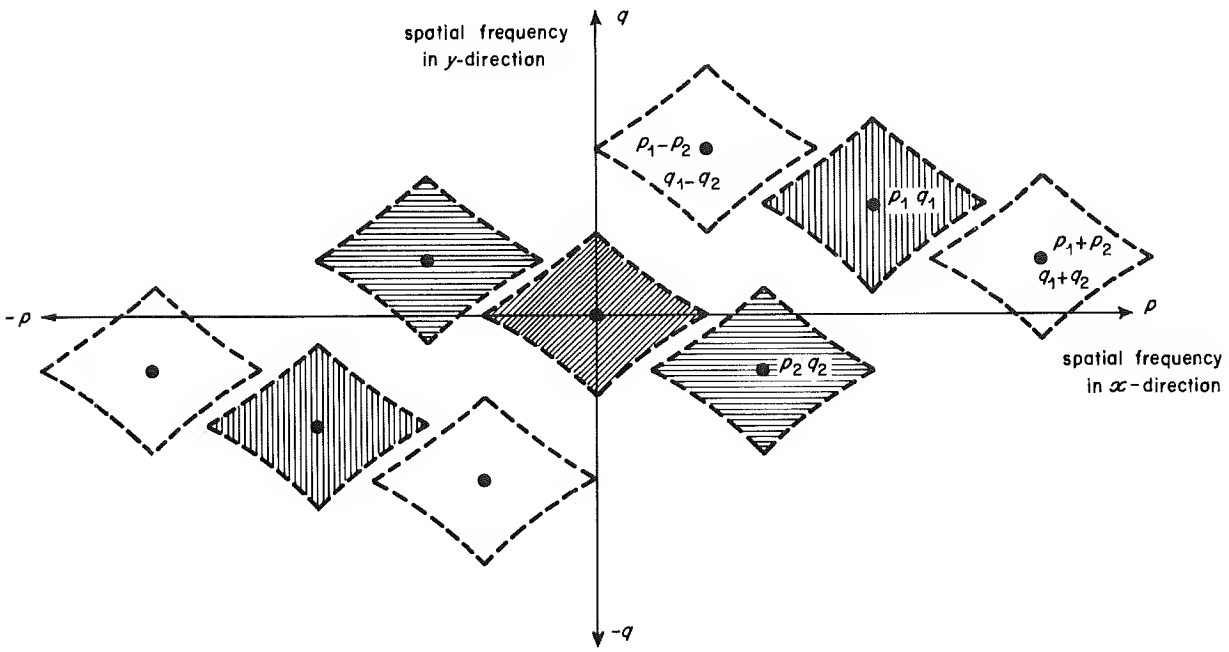

Fig. 3 - Spatial-frequency diagram for a scene encoded by two gratings in tandem. (Same values of p and q as used in Fig. 2)

are proportional to the colorimetric tristimulus values of the scene respectively, e.g. the normal red, green and blue components or linear transformations thereof; and either

(2) the spatial frequencies of the principal carriers are chosen so that their associated sideband spectra do not overlap significantly, either mutually or with the spectrum of the image of the original scene, or

(3) the spatial frequencies of the principal carriers are identical but phased in quadrature. In this case the sidebands must not overlap significantly with the scene spectrum.

Only if the conditions (2) or (3) are fulfilled will it be possible in principle to recover the required separation signals independently by filtering and demodulation techniques. Satisfying the requirement (1) above relies on a judicious specification and control of the spectral response characteristics of the multilayer coatings forming the dichroic gratings, i.e. on the form of variation with wavelength of the functions $A(\lambda)$ and $B(\lambda)$ in Equation (4).

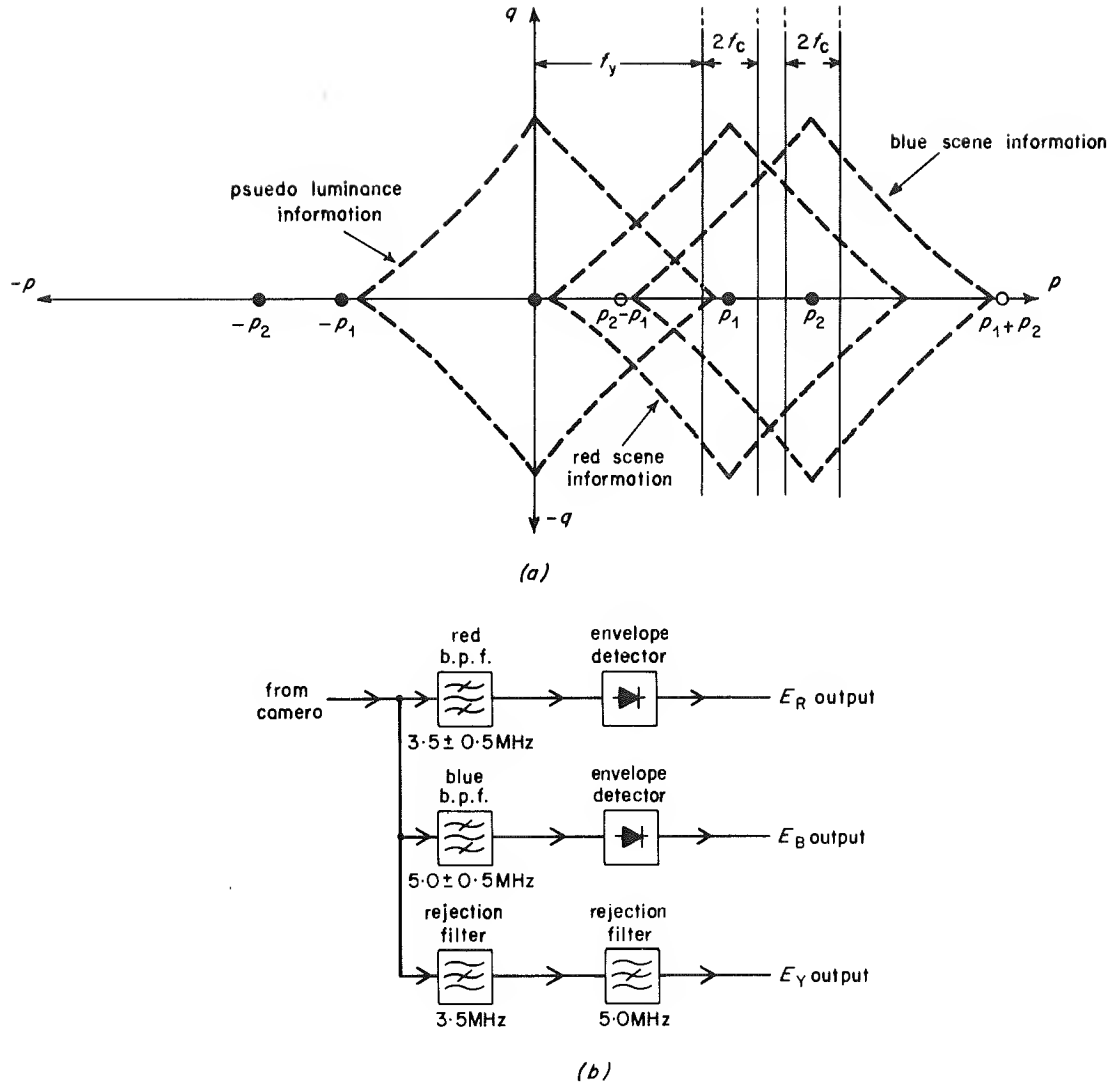

Fig. 4 - R.C.A. encoding and retrieval arrangement

(*a*) Spatial-frequency diagram of encoded scene;
— — — indicates (arbitrarily) extent of scene spectrum O unwanted components (side-band spectra not shown)
(*b*) Simplified version of retrieval filtering arrangement

3. Application in single-tube colour television cameras

3.1. Signal separation methods

Suppose now that the spatially encoded image of the scene is allowed to fall on the target of a television pick-up tube and then scanned in the normal interlaced manner. Three colour-separation signals (e.g. red, green and blue) are required to be derived from the signal output of the tube by suitable electrical filtering techniques and linear matrixing. It will be assumed for the moment that the pick-up tube characteristics are perfect and that the direction of line scan is parallel to the x co-ordinate axes.

Of the several possible approaches, the method discussed by Briel[1] (R.C.A.) is perhaps the most straightforward. Fig. 4(*a*) shows the spatial-frequency diagram of the encoding process, while Fig. 4(*b*) shows a simplified version of the electrical filtering arrangement used for signal retrieval. In this method the fundamental spatial frequencies of the gratings in the line-scan direction, p_1 and p_2, are sufficiently different to enable two (narrow band) signal components to be separated by ordinary electrical band-pass filtering, followed by envelope demodulation. The carrier p_1 is associated with the red information in the scene and p_2 is associated with the blue information. Rejection filters centred on the carrier frequencies (see Fig. 4(*b*)) are used to obtain a wide-bandwidth signal (effectively 3·5 MHz wide with strong attenuation at the carrier frequencies) which forms a pseudo-luminance signal.

If a spatial bandwidth $2f_c$ is ascribed to each of the red and blue separation channels and f_y to the pseudo-luminance channel then it may be seen from Fig. 4(*a*) that in theory the conditions $p_1 \geqslant f_c + f_y$ and $p_2 - p_1 \geqslant 2f_c$ are required to avoid crosstalk between the three separated channels. Moreover, the spatial frequency spectrum of the image of the scene must also be limited to approximately the above values (at least in the line-scan direction) by

optical spatial filtering. (The latter subject is outside the scope of this report but suffice it to say that such filtering although possible, using split-image techniques[3,4] for example, would be difficult to implement especially if different bandwidth restrictions are required for each of the three components). It is worth noting that in the R.C.A. method it is not essential that the red and blue carriers lie on the p-axis (as shown in Fig. 4(*a*)), which means that the dichroic gratings can be orientated with respect to the line-scan direction to obtain the desired spatial frequencies p_1 and p_2.

An alternative encoding method[3,4] allows the spatial frequencies of the gratings to be equal in the line-scan direction but precisely separated in the orthogonal direction as shown in the frequency diagram of Fig. 5(*a*). As in the previous method, a wide-bandwidth pseudo-luminance signal can be separated from the output signal of the pick-up tube by means of a suitable low-pass filter and/or rejection filter. However, electrical processing which produces a band-pass filtering effect in the q-axis direction is required in order to separate out the remaining red and blue signal components. One basic arrangement,[4] shown in Fig. 5(*b*) makes use of a one-line delay and this circuit can be shown to give rise to the filtering characteristics indicated in Fig. 5(*c*). It is instructive to analyse the delay-line circuit shown, with reference to the combined dichroic gratings specified by Equation (4).

Suppose that the incident scene is a spectral colour of wavelength λ, uniform in intensity over the image area, and consider the signal outputs of the n^{th} and $(n+1)^{th}$ scanning lines which traverse the straight lines $y = y_n$ and $y = y_{n+1}$ respectively. Let v be the line-scan velocity and $E(t)$ be the output voltage of the pick-up tube. Then for the n^{th} line we can write

$$E(t)_n = S(\lambda)\, T_1(vt, y_n, \lambda)\, T_2(vt, y_n, \lambda) \tag{5}$$

and similarly for the $(n+1)^{th}$ line

$$E(t)_{n+1} = S(\lambda)\, T_1(vt, y_{n+1}, \lambda)\, T_2(vt, y_{n+1}, \lambda) \tag{6}$$

where $S(\lambda)$ is the sensitivity of the pick-up tube. Using a delay of one scanning line duration, these outputs are made available simultaneously and the following sum and difference signals are formed (Fig. 5(*b*)):

$$E_1(t) = \tfrac{1}{2}[E(t)_n + E(t)_{n+1}] \tag{7}$$

$$\text{and } E_2(t) = \tfrac{1}{2}[E(t)_n - E(t)_{n+1}] \tag{8}$$

Substituting from Equations (4), (5) and (6) we obtain

$$\begin{aligned}\frac{1}{S(\lambda)}E_1(t) = {} & A_1(\lambda)A_2(\lambda) + A_2(\lambda)B_1(\lambda)\cos(2\pi q_1\Delta y)\cos[2\pi(p_1 vt + q_1\bar{y})] \\ & + A_1(\lambda)B_2(\lambda)\cos(2\pi q_2\Delta y)\cos[2\pi(p_2 vt + q_2\bar{y})] \\ & + \tfrac{1}{2}B_1(\lambda)B_2(\lambda)\cos[2\pi(q_1+q_2)\Delta y]\cos\{2\pi[(p_1+p_2)vt + (q_1+q_2)\bar{y}]\} \\ & + \tfrac{1}{2}B_1(\lambda)B_2(\lambda)\cos[2\pi(q_1-q_2)\Delta y]\cos\{2\pi[(p_1-p_2)vt + (q_1-q_2)\bar{y}]\}\end{aligned} \tag{9}$$

$$\begin{aligned}\text{and } \frac{1}{S(\lambda)}E_2(t) = {} & A_2(\lambda)B_1(\lambda)\sin(2\pi q_1\Delta y)\sin[2\pi(p_1 vt + q_1\bar{y})] \\ & + A_1(\lambda)B_2(\lambda)\sin(2\pi q_2\Delta y)\sin[2\pi(p_2 vt + q_2\bar{y})] \\ & + \tfrac{1}{2}B_1(\lambda)B_2(\lambda)\sin[2\pi(q_1+q_2)\Delta y]\sin\{2\pi[(p_1+p_2)vt + (q_1+q_2)\bar{y}]\} \\ & + \tfrac{1}{2}B_1(\lambda)B_2(\lambda)\sin[2\pi(q_1-q_2)\Delta y]\sin\{2\pi[(p_1-p_2)vt + (q_1-q_2)\bar{y}]\}\end{aligned} \tag{10}$$

where $\Delta y = (y_{n+1} - y_n)/2$ and $\bar{y} = (y_{n+1} + y_n)/2$.

According to the encoding method shown in Fig. 5, we set $p_1 = p_2 = p$, $q_1 = 0$, and $q_2 = 1/4\Delta y$. In this case, Equations (9) and (10) reduce to

$$\frac{1}{S(\lambda)}E_1(t) = A_1(\lambda)A_2(\lambda) + A_2(\lambda)B_1\cos(2\pi pvt) \tag{11}$$

$$\begin{aligned}\text{and } \frac{1}{S(\lambda)}E_2(t) = {} & \tfrac{1}{2}B_1(\lambda)B_2(\lambda)\sin(\pi\bar{y}/2\Delta y) + A_1(\lambda)B_2(\lambda)\sin[2\pi(pvt + \bar{y}/4\Delta y)] \\ & + \tfrac{1}{2}B_1(\lambda)B_2(\lambda)\sin[2\pi(2pvt + \bar{y}/4\Delta y)]\end{aligned} \tag{12}$$

Finally, these outputs are passed through band-pass filters of centre frequency pv and the second terms extracted which, after linear envelope demodulation, produce the outputs

$$E_1 = k_1 S(\lambda) A_2(\lambda) B_1(\lambda) \quad (13)$$

and $$E_2 = k_2 S(\lambda) A_1(\lambda) B_2(\lambda) \quad (14)$$

where k_1 and k_2 are variable gain factors independent of wavelength. The third output required is obtained by direct electrical filtering of the signal $E(t)_{n+1}$ (Equation (6)) and produces

$$E_3 = k_3 S(\lambda)[A_1(\lambda) A_2(\lambda) + \tfrac{1}{2} B_1(\lambda) B_2(\lambda) \cos(\pi y_{n+1}/2\Delta y)] \quad (15)$$

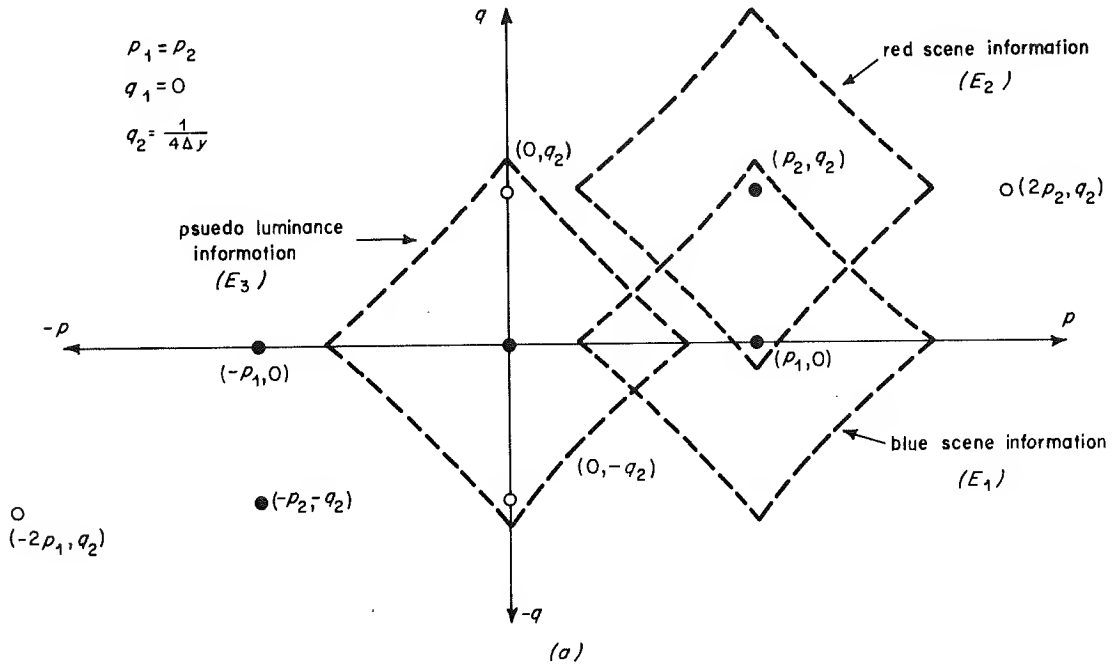

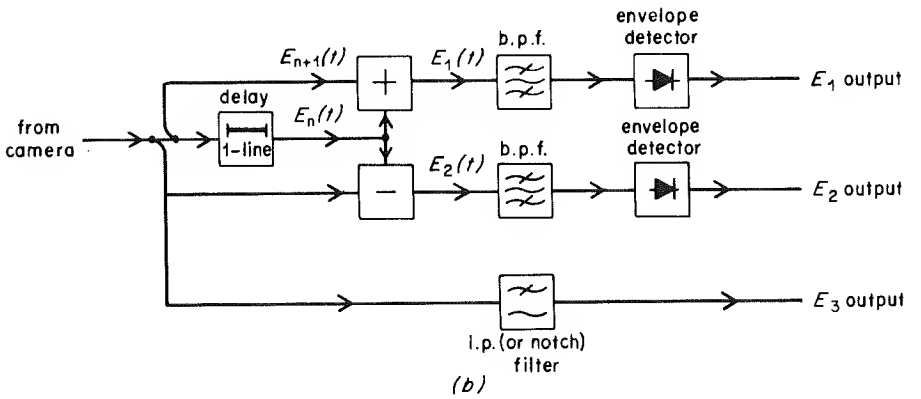

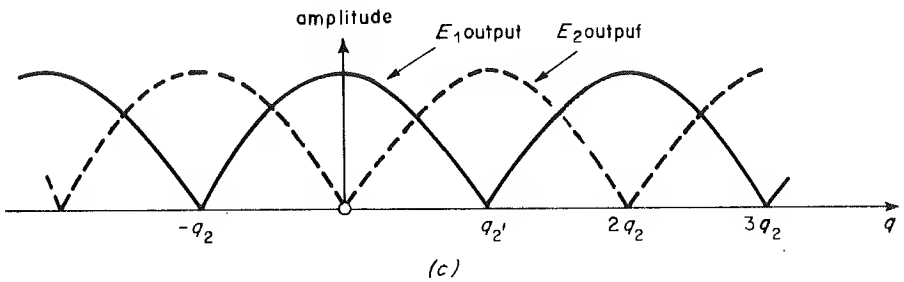

Fig. 5 - Alternative encoding and retrieval process

(*a*) Spatial-frequency diagram of encoded scene;
– – – indicates (arbitrarily) extent of scene spectrum O unwanted components (side-band spectra not shown)
(*b*) Retrieval filtering (*c*) Filtering characteristics of the one-line delay circuit shown at (*b*)

The last term in Equation (15) is seen to be a cosinusoidal function of the vertical scan position. It represents, in fact, an undesirable modulation product which is a fundamental consequence of using two gratings in tandem. A similar term would appear with any encoding method. Fortunately, it can be suppressed by arranging that $B_1(\lambda)$ and $B_2(\lambda)$ are mutually exclusive functions, so that the product $B_1(\lambda)B_2(\lambda)$ is substantially zero for all wavelengths.

To simplify the analysis of the separation of the E_1 and E_2 signals, it was assumed initially that the incident scene was a uniform field. This assumption, however, hides a possible shortcoming of the single delay-line method of filtering just discussed. A more complete analysis would show, in fact, that spatially periodic components of the incident scene in the q-axis direction give rise to cross-talk terms in the E_1 and E_2 outputs whose relative amplitudes are almost directly proportional to the original spatial frequency. This possibility is readily appreciated from the filtering characteristics of the delay-line circuit shown in Fig. 5(*c*). Moreover, Equations (9) and (10) indicate that additional cross-talk effects would arise from systematic variations in the spacing of the scanning lines (hitherto assumed constant) or, more generally, if there is a significant departure from the condition $q_2 = 1/4\Delta y$, where $2\Delta y$ is the line spacing (viz. Section 4.2.1). Hence the method appears to be rather prone to the generation of interfering moiré patterns and colour fringing at horizontal edges. These effects would be mitigated to a greater or lesser extent by

(i) increasing the separation of the spatial frequencies of the carriers in the q direction; for example by setting $q_2 - q_1 = 3/4\Delta y$. Although this would not reduce the maximum amplitudes of the moiré patterns their spatial frequencies would be considerably increased and their visibility thereby diminished;

(ii) using more than one delay-line in the circuit tc produce a more favourable filtering characteristic;

(iii) using a whole field-plus-one-line delay and operating on successive 'picture' lines, with an appropriate adjustment of the $q_2 - q_1$ frequency separation. (This could give rise to movement 'twitter'.)

(iv) modifying the original scene spectrum in the vertical direction by spatial filtering.[3]

3.2. Colorimetric requirements

The grating parameters $A(\lambda)$ and $B(\lambda)$ used in the previous analysis are not independent because both are related to the maximum and minimum transmission coefficients. It may be shown (see Fig. 10(*a*)) that for a grating profile with an equal mark-to-space ratio

$$\frac{B(\lambda)}{c} = \tfrac{1}{2}\left[T_{max}(\lambda) - T_{min}(\lambda)\right] \qquad (16)$$

$$\text{and } A(\lambda) + \frac{B(\lambda)}{c} = T_{max}(\lambda) \qquad (17)$$

where c is a constant depending on the form of the cyclic variation in transmission between the values $T_{max}(\lambda)$ and $T_{min}(\lambda)$. In an ideal grating both c and $T_{max}(\lambda)$ would be independent of wavelength. Thus, assuming an ideal grating and putting $T_{max} = 1$ we have the relation

$$A(\lambda) + \frac{B(\lambda)}{c} = 1 \qquad (18)$$

Substituting for $A_1(\lambda)$ and $A_2(\lambda)$, using the relation (18), in the expressions for the signal outputs E_1, E_2 and E_3 already obtained (Equations (13), (14) and (15)) leads to

$$E_1 = k_1 S(\lambda)\,[B_1(\lambda) - (B_1(\lambda)B_2(\lambda)/c_2)] \qquad (19)$$

$$E_2 = k_2 S(\lambda)\,[B_2(\lambda) - (B_1(\lambda)B_2(\lambda)/c_1)] \qquad (20)$$

$$\text{and } E_3 = k_3 S(\lambda)\,[1 - (B_1(\lambda)/c_1) - (B_2(\lambda)/c_2) +$$

$$+ (B_1(\lambda)B_2(\lambda)/c_1 c_2) + \tfrac{1}{2}B_1(\lambda)B_2(\lambda)\cos(\pi y_{n+1}/2\Delta y)] \qquad (21)$$

The need to arrange that the product $B_1(\lambda)B_2(\lambda)$ is substantially zero for all wavelengths, in order to eliminate the interfering cosine term in the E_3 output, has already been discussed. Invoking this condition thus leads finally to the set of equations

$$E_1 = k_1 S(\lambda)B_1(\lambda) \qquad (22)$$

$$E_2 = k_2 S(\lambda)B_2(\lambda) \qquad (23)$$

$$\text{and } E_3 = k_3 S(\lambda)[1 - (B_1(\lambda)/c_1) - (B_2(\lambda)/c_2)] \qquad (24)$$

for the decoded signal outputs.

The problem now is to choose or prescribe the functions $S(\lambda)$, $B_1(\lambda)$ and $B_2(\lambda)$ so that the variation of the three outputs with wavelength, or a linear transformation of the outputs, approximates to the ideal spectral distribution coefficients for the reproducer primaries. For example, an ideal (peak normalised) set of distribution coefficients ($\bar{r}, \bar{g}, \bar{b}$) for the System I phosphors is shown in Fig. 6. One obvious starting point is to choose $S(\lambda)B_1(\lambda)$ to match the major positive lobe of the $\bar{b}$ function, and $S(\lambda)B_2(\lambda)$ to match the major positive lobe of the $\bar{r}$ function.

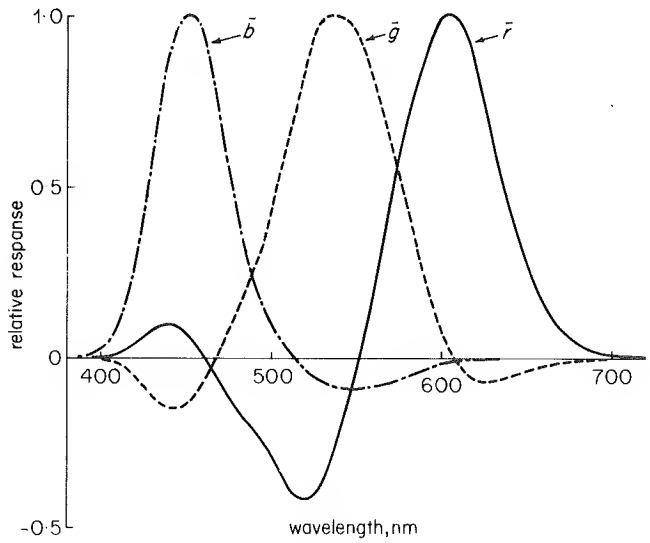

Fig. 6 - Ideal camera analysis characterisitcs for System I phosphors (Illuminant D_{65})

—— Red channel - - - - Green channel —·— Blue channel

Fig. 7(*a*) shows the typical spectral sensitivity of a red-sensitive Plumbicon tube and this response can be 'shaped' to some extent by means of optical colour filters to synthesise, for example, the $S(\lambda)$ function shown in Fig. 7(*b*). Using the latter, in combination with the idealised spectral transmission characteristics $T(\lambda)_{min}$ of the pair of dichroic gratings shown in Fig. 7(*c*), gives rise to the overall spectral responses of the E_1, E_2 and E_3 outputs shown in Fig. 7(*d*). The dashed-line curves of Fig. 7(*d*) are the major positive lobes of the $\bar{r}$, $\bar{g}$ and $\bar{b}$ set of ideal distribution functions, and these are included for comparison. It will be seen that the E_1 and E_2 outputs have been reasonably well matched to the $\bar{b}$ and $\bar{r}$ functions, respectively. However, the spectral response of the E_3 output is much too broad in comparison with the $\bar{g}$ function. The next step, therefore, is to consider the possibility of obtaining a new E_3 output by a linear matrixing operation. For example, Fig. 7(*e*) shows the effect of applying the transformation $E_3 - 0{\cdot}42E_1 - 0{\cdot}18E_2$ in order to match the $\bar{g}$ function approximately.

In an actual system a more sophisticated matrixing operation would probably be used to simulate the negative lobes of the ideal distribution functions, as well as the shaping of the green signal shown in Fig. 7(*e*).

It appears that there are several colorimetric difficulties inherent in the single-tube colour camera discussed. Some of the important features are:

(1) It may prove rather difficult to achieve a high standard of colour fidelity in large areas, even if the dichroic gratings and pick-up tube are ideal, partly because of the need to maintain the condition that the product $B_1(\lambda)B_2(\lambda)$ is substantially zero. In any event, recourse must be made to matrixing operations with relatively large negative coefficients;

(2) If the E_3 output is a signal having the full video bandwidth and the E_1 and E_2 outputs have greatly reduced bandwidths, the reproduced luminance will be incorrect for medium-and-fine detail in red or blue areas (see Fig. 7(*d*)), and colour fringing at edges may also occur.

(3) The E_1 and E_2 outputs are directly proportional to the modulation transfer coefficient of the pick-up tube at the associated spatial carrier frequencies, so that colour shading in large areas is inevitable if the tube resolution (i.e. effective scanning spot size) is not constant over the picture area.

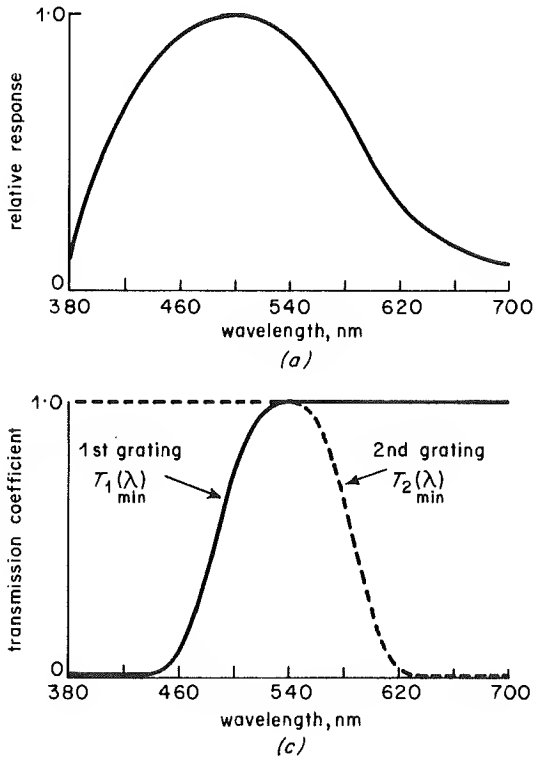

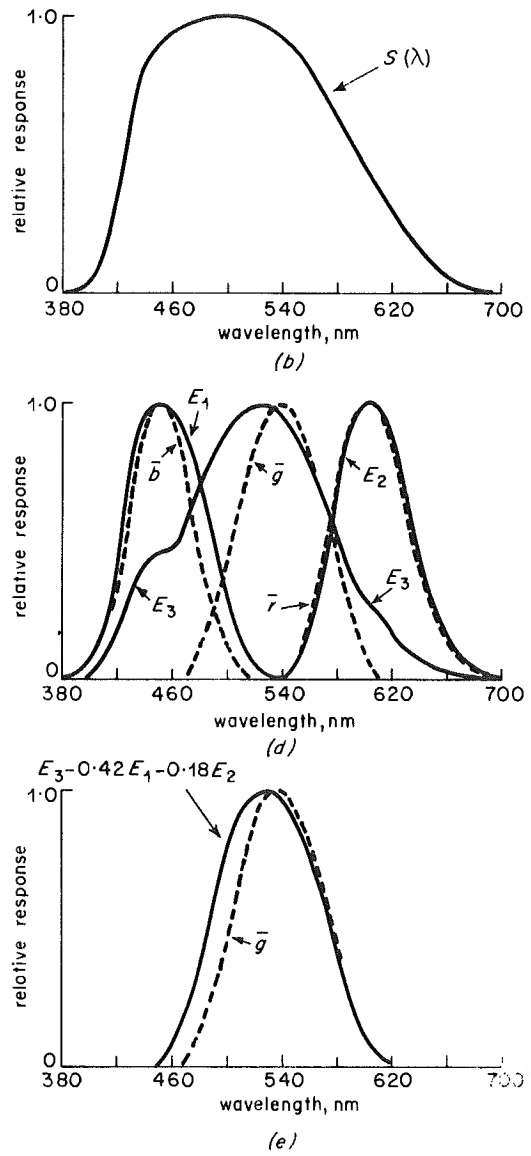

Fig. 7 - Colorimetry associated with single-tube camera using dichroic gratings

(*a*) Typical plumbicon response (red sensitive);
(*b*) 'Shaped' plumbicon response, $S(\lambda)$;
(*c*) Spectral characteristics of ideal gratings;
(*d*) Spectral responses of decoded outputs;
(*e*) Transformation of E_3 output to match $\bar{g}$ function
——— system output
– – – – ideal analysis

4. Constructional tolerances for the grating parameters

Specifying realistic tolerances on the various characteristics of the dichroic gratings is rather difficult, in the absence of direct subjective evidence of several possible deleterious effects due to deficiencies in construction. Moreover, there is some uncertainty regarding the overall standard of performance required from the camera. It has been argued, for example, that because one cannot reasonably expect to achieve the same high standard of performance as that of a modern 3-tube or 4-tube colour television camera, a lower standard might be acceptable for some programmes in exchange for a smaller and cheaper colour camera.

In this section we assume that all the other components in the chain are ideal and attempt to estimate the individual grating tolerances required for a 'fair' standard of performance.

4.1. Spectral characteristics of the multilayer coating

4.1.1. Variation of $T_{min}(\lambda)$ over the picture area

Due to non-uniformity of layer thicknesses in the vacuum deposition process, the spectral characterisitcs of the multilayer could vary systematically over the grating area. The most likely result will be a shift of the $T_{min}(\lambda)$ function with respect to wavelength. If this occurs for one of the pair of gratings, two of the decoded outputs will change by approximately equal fractional amounts but in opposite directions. To estimate the shift tolerances, we suppose that the camera looks at a uniform reference white (Illuminant D_{65}, say) and that the decoded outputs are balanced to reproduce this chromaticity in the centre of the picture. Assuming that the chromaticity towards the edge of the picture should not differ from that at the centre by more than 0·01, C.I.E.-U.C.S. units, then calculations indicate that the E_3 output must not vary by more than about ±8%. Thus the wavelength shift of $T_{min}(\lambda)$ over the used area of each grating should not vary by an amount which alters any output by more than ±4%. Fig. 8 shows these shift tolerance limits applied to the idealised spectral characteristics cited earlier.

4.1.2. Violation of the condition $B_1(\lambda)B_2(\lambda) = 0$

As Equation (4) indicates, a static interference pattern is generated if we cannot ensure that the product $B_1(\lambda)B_2(\lambda)$ is zero. In terms of the $T_{min}(\lambda)$ function, the magnitude of the interference is reduced by arranging that the transmission coefficient of one grating is as large as possible over that spectral region where the transmission coefficient of the second grating is least, and vice versa. The visibility of the interference pattern will depend both on its spatial frequency and the relative fluctuation in luminance it causes. The latter will in turn depend on the transmitted colour, and is expected to be greatest for saturated blue and red colours. If we can regard a relative fluctuation in luminance of ±2% or less to be tolerable, then the $T_{min}(\lambda)$ function should exceed 92% in the most sensitive regions. This lower limit is indicated also in Fig. 8.

In order to achieve the required characteristic, it will be necessary to include 'smoothing' layers in the multilayer design to suppress the fluctuations in the transmission band which are a well-known feature of dichroic filters.

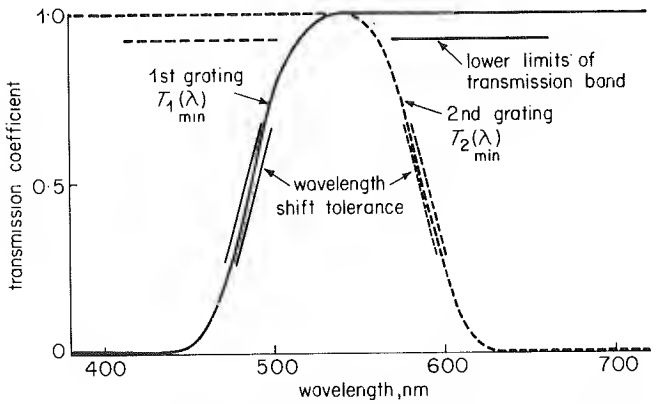

Fig. 8 - Variational tolerances applied to ideal-grating spectral characteristics

4.2. Grating geometry

Two other constructional imperfections, which may lead to objectionable effects, are systematic variations in the spatial frequency and in the transmission profile over the used area of the grating.

4.2.1. Variation of spatial frequency

A systematic variation of spatial frequency may be caused by a lack of parallelism (wedge effect) or by curvature of the coated stripes. The effect on the reproduced picture of such a frequency variation will depend on the particular encoding method used. In those systems which require only a spatial 'carrier' component in the line-scan direction, the permissible deviation in carrier frequency is related to the bandwidth, W, of the bandpass filters used to isolate the E_1 and E_2 outputs. Assuming that we could allow deviations in carrier frequency up to ±6% of the filter bandwidth, then the corresponding tolerance on the relative deviation in carrier frequency is

$$\frac{\Delta f}{f} < 0{\cdot}06(W/f)$$

where f is the carrier frequency and Δf the deviation. Relating this tolerance to the permissible curvature of the stripes we obtain the condition

$$|\Delta\theta| < 0{\cdot}06(W/f)\cot\theta$$

where θ is the (mean) orientation of the grating stripes with respect to the direction orthogonal to the line-scan, and $|\Delta\theta|$ is the maximum deviation in stripe direction over the grating area.

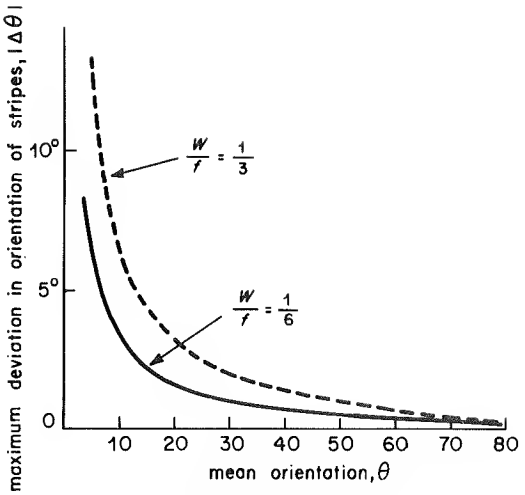

Fig. 9 - Tolerances for stripe curvature

Fig. 9 shows a plot of the limiting value of $|\Delta\theta|$ as a function of the mean orientation θ for two values of the parameter (W/f). The figure illustrates the rather obvious fact that stripe curvature is not important when θ is small.

If the alternative encoding method[3,4] is used, then an additional effect arises from variations of spatial frequency in the direction orthogonal to the line-scan. There exists a strong probability of significant cross-talk between the E_1 and E_2 outputs producing a local moiré-type interference. It is calculated that a 2% deviation in the frequency of one spatial carrier will result in approximately 3% of the amplitude of that carrier appearing in the other output.

4.2.2. Variation in mark-to-space ratio

A possible source of error is associated with the constancy of the factor c in Equations (16) and (17). For example, the full-line in Fig. 10(*a*) shows the square-wave transmission profile, at a given wavelength, for a grating designed to have alternate stripes of coated and uncoated glass with a 1 : 1 mark-to-space ratio. The dashed-line shows the fundamental Fourier component of this profile and its amplitude is $B(\lambda) = c[T_{max}(\lambda) - T_{min}(\lambda)]/2$ as indicated in the figure. However, if the mark-to-space ratio changes, the amplitude will diminish at the rate shown in Fig. 10(*b*), where the factor c is plotted as a function of mark-to-space ratio. Hence $B(\lambda)$ diminishes, and reference to the set of Equations (22) to (24) shows that either or both of the decoded outputs, E_1 and E_2, will be reduced but not the E_3 output. Using again the criterion that the colour balance on a reference white should not vary by more than 0·01 C.I.E.-U.C.S. units, it can be shown that the E_1 and E_2 outputs should not vary by more than ±8%, approximately. Hence a deviation of mark-to-space ratio from 1 : 1 to 4 : 7 would be permissible (see Fig. 10(*b*)). This is equivalent to a tolerance of ±25% in the width of the coated stripe, which could easily be met in practice.

5. Constructional techniques

For application in single-tube colour cameras, maximum spatial frequencies in the range 10 to 25 cycles/mm, and

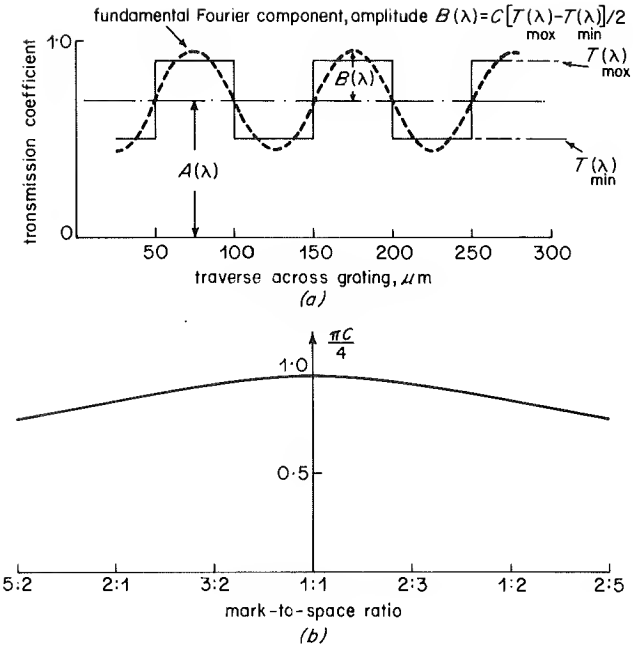

Fig. 10 - Effects of variations of mark-to-space ratio

(*a*) Square-wave transmission profile at a 1 : 1 mark-to-space ratio;
(*b*) Variation of $B(\lambda)$ with mark-to-space ratio, for square-wave profile.

grating areas in the region of 200 sq. mm, would represent a practical requirement. Constructional techniques should be developed, therefore, to produce coated stripe widths in the range 20 to 50 μm. The ideal solution would be to deposit the dichroic gratings directly on to the inside surface of the pick-up tube faceplate and then overlay the photo-conductive coating. However, the latter possibility is beyond the scope of this note and it is assumed here that the individual gratings are to be separately formed on polished glass substrates, brought almost into mutual contact and the assembly then placed in the first image plane of the optical system.

There are two alternative approaches to the construction. One could either deposit the stripes directly on to the substrate by vacuum evaporation through a suitable open mask or grille, or vacuum deposit over the whole surface and then remove stripes of the coating leaving clear spaces. In the former approach the problem is to fabricate a self-supporting grille and to hold it firmly in close contact with the glass substrate during the evaporation. One method (which has in fact been used successfully for much wider stripes) is to wind a frame of fine-drawn wire and remove every other turn. The substrate is rested on the wire grille so formed and evaporation takes place from underneath, as shown in Fig. 11(*a*). An alternative method, which provides a larger surface area of contact with the substrate, is to fabricate the open mask in thin but stiff metal foil (e.g. molybdenum foil) by means of photoresist and etching techniques. The problem of holding the masks in close contact with the substrate could be solved by constructing the mask from a magnetic material and placing permanent magnets on the opposite side of the substrate.

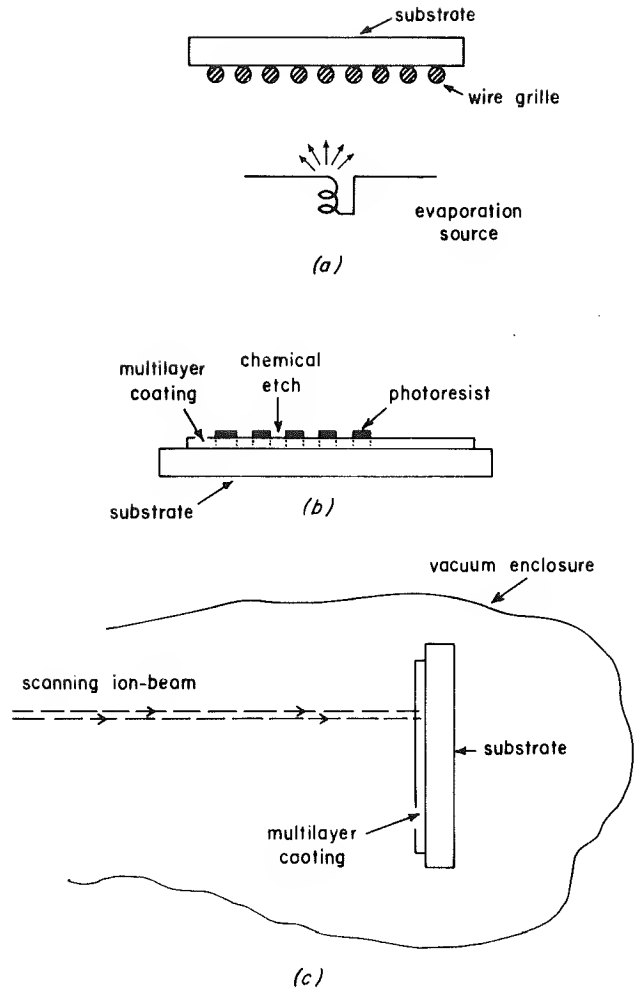

Fig. 11 - Possible constructional techniques for dichroic gratings

(*a*) Open-mask technique; (*b*) Photoresist and chemical etch; (*c*) Ion-beam sputtering

The second approach, in which the whole substrate is coated and then stripes of material removed (Fig. 11(*b*)), has the advantage that the spectral characteristics of the multilayer are more easily controlled and monitored during the initial evaporation process. On the other hand, removal of the coating in narrow stripes by photoresist and chemical etching techniques could prove difficult, partly because a combination of different dielectric materials is used for the multilayer. Indeed, it may prove necessary to select the dielectric materials to suit the etch process.

Another possible method of removal, suggested by Holland,[5] is to place the coated substrate in a vacuum chamber and slowly scan it with a focussed ion beam, as illustrated in Fig. 11(*c*). The removal action is due to the back sputtering of material which takes place wherever the ion beam has impinged. At the present time, however, precision ion-beam sputtering is at an early stage of development.

6. Conclusions

The analysis of the encoding action of a pair of dichroic gratings, and of the application to a single-tube colour television camera, has revealed several of the problems associated with the process of information retrieval. The choice of encoding method and the filtering processes, both optical and electrical, required for retrieval are important factors if significant cross-talk between the three outputs are to be avoided.

Apart from cross-talk effects and colour shading, which are likely to arise mainly from tube scanning non-linearity and variations in effective spot size, the basic colorimetry could be made reasonably accurate by paying sufficient attention to the spectral characteristics of the gratings and the other components in the chain. Linear matrixing of the outputs is required and, for the best results, a special colour-correcting filter will probably be required in addition.

Approximate tolerances have been derived for several parameters of the dichroic gratings (viz. Section 4), but some of these tolerances may need revising if there are unavoidable, systematic errors in the electrical scanning process.

It is concluded that dichroic gratings which meet the particular tolerances estimated here could be produced with perhaps only a modest amount of development effort.

7. References

1. BRIEL, L. 1969. A single-vidicon television camera system. *J. Soc. Motion Pict. Telev. Engrs*, 1970, **79**, 4, pp. 326 – 330.

2. MULLER, P.F. Colour image retrieval from monochrome transparances. *Appl. Optics*, 1969, **8**, 10, pp. 2051 – 2057.

3. RAINGER, P. British Patent Specification No. 58549/69.

4. BBC Designs Department Technical Memorandum No. 7.162(70).

5. HOLLAND, L. Edwards high vacuum. Private communication.

Printed by BBC Research Department, Kingswood Warren, Tadworth, Surrey